

MEAN AND FLUCTUATING PRESSURE MEASUREMENTS IN A PASSIVE CONTROLLED SHOCK BOUNDARY LAYER INTERACTION.

S. Raghunathan,  
Department of Aeronautical Engineering,  
The Queen's University of Belfast,  
Belfast, Northern Ireland.

Abstract

The concept of passive shockwave boundary layer (PSBL) control in transonic flow and the research investigations in this area to date, both experimental and theoretical, are discussed. It is shown that PSBL control on a transonic aerofoil can produce an increase lift, reduction in drag and pressure fluctuations and improve the buffet boundaries.

The aim of this paper is to analyse the experimental investigations on PSBL performed at Queen's University, Belfast in relation to the work done primarily at Rensselaer Polytechnic Institute, New York and DFVLR, Gottingen. The theoretical predictions of NASA Ames are also discussed.

Nomenclature

$C_p$	pressure coefficient
$C$	model chord length
$d$	hole diameter, slot width
$f$	frequency
$\sqrt{nF(n)}$	forcing function
$M_{SO,\infty}$	shock Mach number at zero porosity, free stream Mach number
$n$	frequency parameter $fc/U_\infty$
$p$	porosity open area/model area
$\bar{p}$	RMS pressure fluctuations
$q_\infty$	free stream dynamic pressure
$Re$	Reynolds number $U_\infty c/\nu$
$U_\infty$	free stream velocity
$x_{SO,T}$	shock position, transducer position
$x_p$	position of the porous surface
$y$	distance normal to the chord
$\delta^*$	boundary layer displacement thickness
$\nu$	kinematic viscosity of air

1. Introduction

The transonic flow over aerofoils contains a region of supersonic flow embedded in a subsonic flow. The supersonic region terminates in a shock wave and depending on the strength of the shock-wave the boundary layer on the surface of an aerofoil may separate with or without reattachment (Fig. 1a). The information of shock waves and the associated flow separation leads to a significant increase in drag. The techniques to postpone the free stream Mach number at which the drag rise occurs include the use of swept back or swept forward wings, thin aerofoils, low aspect ratio wings, boundary layer control on the wind surface by suction/blowing and by vortex generators, application of area rule technology to aircraft design and supercritical wing technology.

The supercritical wing which is designed to produce relatively weak shock waves on the wing is aerodynamically efficient at the design Mach number and the drag increases rapidly with the Mach number at off design conditions.

A novel concept of drag reduction in transonic flow is the passive shock wave boundary layer control (PSBL) at the foot of the shock and

2. The Concept of passive shock wave boundary layer control

The concept of passive shock wave boundary layer control consists of a porous surface and a plenum at the foot of the shock wave. The natural static pressure rise across the shock wave causes a flow through the plenum from downstream to upstream of the shock wave (Fig. 1b) altering the effective geometry resulting in weaker shock waves which in turn reduces the entropy change across the shock. The weaker waves and the flow into the plenum downstream of the shocks also reduce flow separation.

3. Investigations

Both the experimental<sup>1-5</sup> and theoretical<sup>6,7</sup> investigations performed to date have shown that the PSBL does work. These investigations are tabulated in Table 1. It appears from these investigations that the controlling parameters for the PSBL are (1) relative position of shock wave and porous region, (2) type of porous surface-this could be normal or inclined holes to the surface, single or multiple slots, (3) strength of porosity, (4) distribution of porosity-could be constant (type A) varying with the maximum porosity at the shock position (type B) or maximum porosity at the mid position of the porous region (type C), and (5) the width and depth of the plenum chamber.

The earlier work of Nagamatsu et al<sup>1,2</sup> was performed in a porous wall tunnel which was subsequently modified with a contoured wall to increase the range of Mach number. The work done at Rensselaer Polytechnic<sup>1,2</sup> and Queen's University<sup>3</sup> were on wall mounted models in small transonic wind tunnels whereas the experiments at DFVLR<sup>4,5</sup> were conducted on a lifting aerofoil in a larger tunnel (Fig. 2). The wall mounted model in the RPI tunnel had boundary layer bleed whereas the model in the QUB tunnel had thick boundary layer growing on the tunnel walls with a value of  $R_\theta \approx 10^4$  at the foot of the shock which is comparable to the boundary layer conditions on models in larger tunnels. The shock Mach numbers for all the investigations were in the range 1.2 - 1.4. The types of porous surfaces tested were normal holes (NH), forward facing holes (FFH) and backward facing holes (BFH) on the model surface and slots, single and double. All the experiments have been done with a uniform porosity distribution (type A). The theoretical

investigations<sup>6,7</sup> included the varying porosity distributions type B and C. The porosity strengths were in the range 0.15 - 2.8%. The ratio of the diameter of holes to the boundary layer displacement thickness  $d/\delta^*$  may be an important parameter and this was in the range 0.15 - 3.

#### 4. Effect of porosity and strength

The effect of porosity on a model surface is to reduce the pressure gradients on the model as seen from Figs. 3 a - c. For a porous surface with normal holes the effect of porosity is to decrease the negative  $C_p$  values near the leading edge of the porous surface and to increase the negative  $C_p$  near the trailing edge of the porous surface (Fig. 3a). The Mach number distributions<sup>1,2</sup> obtained on supercritical aerofoil (Fig. 3b) also show similar effect of porosity. The inclined holes, however, produce a general reduction of negative  $C_p$  values over the porous region (Fig. 3c). Clear differences in  $C_p$  distribution between the solid model and the corresponding porous model show the change in the effective geometry of the surface and this must be due to a recirculating air flow. The porous surface with the plenum should also increase the communication between the two sides of the shock wave which in turn should have the effect of reducing the pressure gradients in the shock boundary layer interaction region in a way similar to that in a laminar boundary layer shock wave interaction except that the boundary layer on the surface here is turbulent and therefore less vulnerable to separation. The effect of increasing the porosity will have two opposite effects. The increase in area of porous surface associated with the increase in porosity should increase the recirculating air flow and communication but an increase in the communication across the shock wave should reduce the pressure difference across the shock and therefore the recirculating mass flow.

The structure of the shock wave is changed by the effect of porosity. Wall mounted model experiments show that a single shock wave changes into several weaker shocks with the introduction of porosity. The leading shock of this shock system is an oblique shock anchored to the leading edge of the porous region. The tail end of the shock system is almost a normal shock located either in the porous region (Fig. 4 a,b) or the trailing edge of the porous region and the position of which does not significantly differ from the original shock position on the solids model.

The results of the lifting aerofoil tests<sup>4,5</sup> are less clear. Although, for small incidences, the shock is anchored to a fixed position on the porous surface, the shock moves upstream of the porous surface at relatively larger incidences. For conditions corresponding to a significant drag reduction the control surface is actually downstream of the shock wave and it is difficult to explain the mechanism of drag reduction by the concept of PSBL. (Fig. 4(c).)

The effect of porosity on the boundary layer

on the shock wave can be interpreted from the stagnation pressure measurements in the wake (Fig. 5a,b). Porosity appears to increase the viscous losses, but only slightly, near the surface but reduces the stagnation pressure losses (entropy change) across the shock wave which agrees with the concept that weaker shock waves result from the recirculating flow in the porous region. Some of the experiments of Nagamatsu et al<sup>1,2</sup> have shown that at higher free stream Mach number ( $M_\infty = 0.87$ )

that is with stronger shocks and flow separation, the presence of the porous surface with plenum can also reduce the viscous losses near the surface by suppressing flow separation. Thus it appears that PSBL can reduce both the viscous losses and entropy changes across the shock boundary layer interaction.

#### 5. The inclination of holes

The PSBL control is effected by the type of the porous surface<sup>3</sup> (Fig. 6). The differences in the pressure distributions obtained with normal holes (NH), backward facing holes (BFH) and forward facing holes (FFH) indicate the sensitivity of the PSBL control with the hole inclination. When the results are compared with the solid model NH produces more upstream influence than FFH or BFH. The changes in  $C_p$  values are larger for the inclined holes than for the normal holes. In terms of drag reduction the FFH appear to produce the maximum reduction as seen from Fig. 7 which shows a plot of  $C_D/C_{D0}$ , where  $C_{D0}$  is the drag value for zero porosity model, vs porosity. The optimum porosity for maximum drag reduction appears to be between 2% - 3%. However the experiments on a lifting aerofoil<sup>4,5</sup> with slots suggests that a significant drag reduction can be achieved with a porosity less than 1%.

#### 6. Cavity depth

The effect of cavity depth<sup>1,2</sup> on the PSBL control can be observed from Fig. 8 which shows the Mach number distribution on a wall mounted supercritical aerofoil for two different cavity depths compared with the solid model. Increase in cavity depth tends to reduce the pressure gradients on the model. These experiments showed<sup>1,2</sup> that although the pressure distribution on the surface was affected by the cavity depth the drag reduction was not effected. It has been suggested that to achieve a maximum lift to drag ratio on an aerofoil the cavity depth should be small.

#### 7. The relative position of shock wave and porous region

The relative positions of the shock wave ( $x_{S0}/c$ ) and the region of porosity ( $x_p/c$ ) is important for a maximum drag reduction. Fig. 9 shows the variation of  $C_D/C_{D0}$  with  $M_{S0}$  obtained with a FFH model, for a porosity  $p = 1.6\%$  and for three positions of the porous region  $x_p/c = 0.74 - 0.94$ ,  $0.75 - 0.88$  and  $0.7 - 0.84$ . and for  $p = 4.6\%$  with  $x_p/c = 0.53 - 0.94$ . The results of Ref. 2 with normal holes and Refs. 4, 5 with slots are also shown here for comparison. Referring to the QUB experiments, it is observed that for typical

values of  $M_{SO} = 1.3$  at which  $x_{SO}/c = 0.8$ , and for  $p = 1.6\%$  denser porosity ( $x_p = 0.75 - 0.88$ ) is better than more widely distributed porosity  $x_p/c = 0.75 - 0.94$  and the best results are obtained for  $x_p/c = 0.7 - 0.84$  which corresponds to about 2/3 porosity upstream of the shock wave and 1/3 porosity downstream of the shock. Similar results have also been obtained with normal holes<sup>2</sup>. The results also show that a relatively large porosity ( $p = 4.6\%$ ) distributed over a wider range ( $x_p/c = 0.53 - 0.94$ ) produces relatively smaller reduction in drag. A large reduction in  $C_D/C_{D0}$  obtained with double slots<sup>4,5</sup> and with a small porosity of  $p = 0.3\%$  was with the porous region downstream of the shock wave which is in contradiction to the results of QUB and RPI.

### 8. The type of porosity distribution

The theoretical predictions<sup>6,7</sup> based on potential flow analysis indicate that the PSBL control is governed by the type of porosity distribution. Calculations based on predictions with the varying porosities type B (maximum porosity at the shock position) and type C (maximum porosity at the mid point of the porous region) are compared with the experimental results in Fig. 10. The experimental results were all obtained with type A or with slots. In comparing the theoretical results with the experiments it should be noted that the viscous effects are not included in the predictions.

The type B distribution shows that for a given porosity the drag reduction increases with the increase in the free stream Mach number and for a given free stream Mach number (shock strength) increase in porosity results in a larger drag reduction. This trend agrees with the experimental results with type A porosity distribution. For type C porosity distribution the drag reduction increases with the free stream Mach number only up to a certain free stream Mach number after which the reduction in drag reduces with the increase in free stream Mach number. Very sharp increase in drag reduction with the free stream Mach number obtained with the circular arc model is due to a rapid increase in the shock Mach number with small changes in the free stream Mach number in the tunnel where these tests were conducted. Although the viscous effects were neglected, the results suggest that type B porosity may be a better distribution than the type A porosity for achieving maximum drag reduction.

### 9. Effect on lift

The effect of porosity is not only to decrease drag but also increase lift. Calculated values of  $(C_L/C_D)$  for a porous model normalised with respect to the corresponding value for the solid model are plotted against  $M_\infty$  in Fig. 11. These results, based on potential flow analysis and therefore exclude viscous drag, show that typically at  $M_\infty = 0.78$  the lift to drag ratio for an aerofoil can be doubled with the application of PSBL control.

### 10. Pressure fluctuations and buffeting

There is evidence to show that PSBL control can reduce the pressure fluctuation levels in the shock boundary layer interaction region and therefore extend the buffet boundaries for a wing.

Pressure fluctuation levels  $\tilde{p}$  measurements made by Kulite transducers on a circular arc model with and without PSBL control are shown in Fig. 12. The values of  $\tilde{p}$  are normalised with respect to the free stream dynamic pressure  $q_\infty$ . The results shown here are for a solid model and a model with FFH at  $M_{SO} = 1.30$  and  $x_{SO}/c = 0.8$ .

For the solid model the  $\tilde{p}/q_\infty$  values increase to a maximum value at the shock position but the values are not significantly high (<3%) to indicate any severe shock oscillations. The effect of PSBL is to reduce the  $\tilde{p}/q_\infty$  values considerably at the shock position with a slight increase downstream of it. This suggests that the plenum chamber, which sets up a communication to both sides of the shock wave, acts as a stabilizer for any shock movement. It should be interesting to perform similar investigations in a situation involving strong shock oscillations.

The spectra of pressure fluctuations plotted in the form  $\sqrt{nF(n)}$  vs  $n$ , where,  $\sqrt{nF(n)}$  is the forcing function and  $n$  is the reduced frequency, for  $M_{SO} = 1.3$  and two transducer positions  $x_T/c = 0.78$  and  $0.92$  are shown in Figs. 13(a) and 13(b). It is clear from these figures that the effect of PSBL is to reduce the levels at lower frequencies significantly (<1KHz) and to increase the levels slightly at higher frequencies. The solid surface model shows a peak in spectra at  $n \approx 0.28$  at the shock position. This would correspond to a frequency parameter of  $2\pi fc/U_\infty = 1.13$  which compares well with the other experimental values measured at the shock position. The reduction in the pressure fluctuation levels at low frequencies will also reduce the buffeting associated with oscillations and shock induced separation.

The experiments currently in progress at Queen's University, Belfast suggest that further reduction pressure fluctuation levels can be achieved with inclined holes interconnected by tubes.\*

The measured buffet boundaries for a lifting aerofoil with and without PSBL are shown in Fig. 14. The figure shows that at Mach numbers higher than the design Mach number the buffet boundaries can be increased substantially which does suggest that the excitation force reduces with the PSBL control.

\* This concept is patented jointly by Queen's University and the Ministry of Defence, U.K. Patent application No. 8600175.

## 11. Conclusions

The concept of passive shock wave boundary layer control for drag reduction in transonic flow and the parameters controlling it are discussed in this paper. Theoretical and experimental investigations in this area show that PSBL reduces drag, increases lift and improves buffet boundaries. More investigations are needed to optimise the type of porosity distribution required for maximum drag reduction.

## 12. Acknowledgement

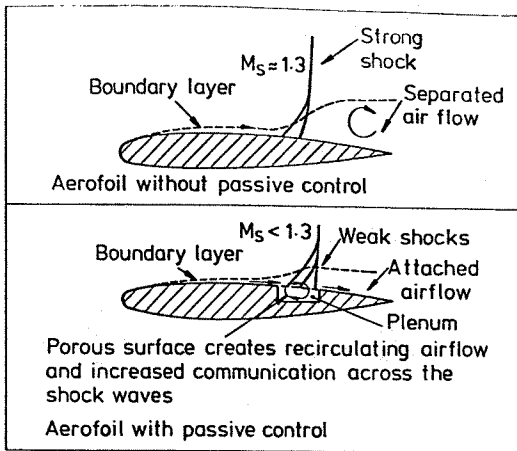
The author wishes to acknowledge the financial support given by SERC for these investigations and also thanks Mr. D.G. Mabey, RAE, Bedford, Mr. D.A. Butter, British Aerospace, Weybridge Division and Mr. F. Ogilvie, British Aerospace, Hatfield, for their useful suggestions.

## 13. References

- Bahi, L., Ross, J.M. and Nagmatsu, H.T., 'Passive shock wave/boundary layer control for transonic aerofoil drag reduction.' AIAA 21st Aerospace Sciences Meeting, Reno (Nev.), Jan. 1983, Paper No. 83 - 0137.
- Nagmatsu, H.T., Dyer, R. and Ficarra, R.V., 'Supercritical aerofoil drag reduction by passive shock wave/boundary layer control in the Mach number range 0.75 - 0.9.' AIAA 23rd Aerospace Sciences Meeting, Reno (Nev.) Jan. 1985. Paper No. 85 - 0207.
- Raghunathan, S. and Mabey, D.G. 'Passive shock wave boundary layer control experiments on a circular arc aerofoil.' AIAA 24th Aerospace Sciences Meeting, Reno (Nev.), Jan. 1986. Paper 86 - 0285.
- Krogmann, P. and Stanewsky, E. 'Effect of local boundary layer suction on shock boundary layer interaction and shock induced separation.' AIAA 22nd Aerospace Sciences Meeting, Reno (Nev.), Jan. 1984. Paper 84 - 0098.
- Theide P. et al, 'Active and passive shock wave/boundary layer control of supercritical aerofoil.' AGARD-FDP Symposium, Brussels, May 1984.
- Savu, G. and Terifu, O. 'Porous aerofoils in transonic flow.' AIAA Journal, Vol. 22, July 1984. pp. 989 - 991.
- Chen, C.L., Chen, Y.C., Holst, L. and Van Daiseem, R. 'Numerical study of porous aerofoils in transonic flow.' NASA TM 86713, May 1985.

Authors	Nagmatsu etl (1,2)	Author 3	Krogmann etl (4,5)	Savu etl (6)	Chen etl (7)
Wind tunnel / analysis	3" x 15" top wall contoured	4" x 4" slotted floor	1m x 1m perforated wall	Potential flow analysis	Potential flow analysis
Model	14% supercritical 4" chord floor mounted	6% circular arc 4" chord roof mounted	13% supercritical 0.2m chord	NACA 0012	NACA 0012
$M_{\infty}$	0.75 - 0.90	0.78 - 0.82	0.7 - 0.8	0.7 - 0.9	0.7 - 0.85
$M_{50}$	- 1.3	1.2 - 1.37	- 1.4		- 1.3
$X_{50}/C$	0.63 - 0.9	0.67 - 0.82	0.5 - 0.6		0.4 - 0.5
$X_P/C$	0.56 - 0.83	0.70 - 0.88	0.55 - 0.62	0.1 - 1.0	0.1 - 0.9
Type of porous surface and distribution	Normal holes Type A	Normal holes inclined holes Type A	Normal holes slots Type A	Normal holes Type C	Normal holes Types B,C
Porosity % (model area)	0.9% - 2.8%	1.6% - 2.9%	0.15% - 0.75% Single Normal slot	0 - 10%	0 - 10%
Porosity % (control area)	10.37%	9% - 16%	4% - 8%	0 - 10%	0 - 10%
$\frac{d}{\delta^*}$	- 3	- 1	0.15 - 0.66 Normal Single holes slot		
Reynolds number	$Re = 2 \times 10^6$ $Re = 0.3 \times 10^4$	$Re = 10^4$	$Re = 2.5 \times 10^6$ $Re = 10^4$		

Table 1. Investigations on PSBL control.



**CONTROLLING PARAMETERS**

1. Relative position of shock wave and porous region
2. Type of porous surface (holes, holes inclinations, slots)
3. Strength of porosity
4. Type of porosity distribution  
 constant :- Type A  
 varying :- Maximum porosity at the shock position - Type B  
                   Maximum porosity at the midpoint - Type C
5. Plenum geometry

Fig. 1. PSBL control concept.

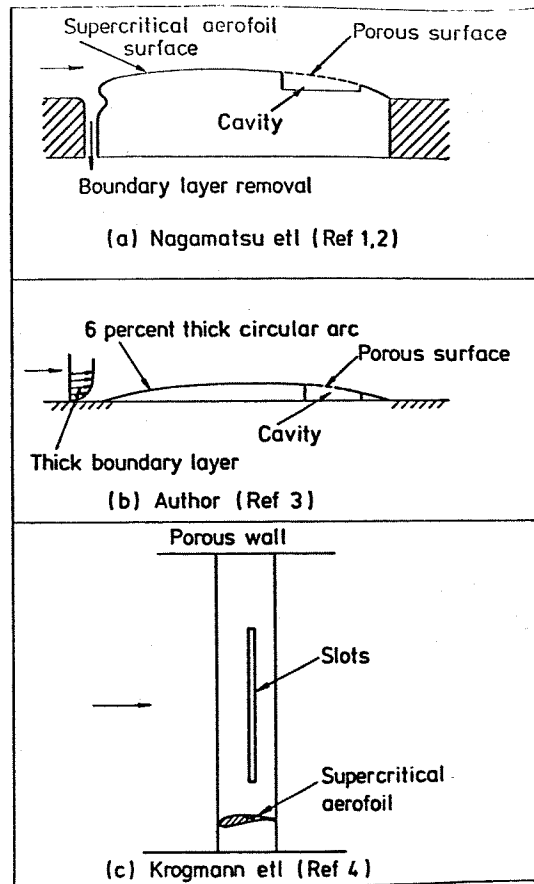


Fig. 2. Types of models investigated.

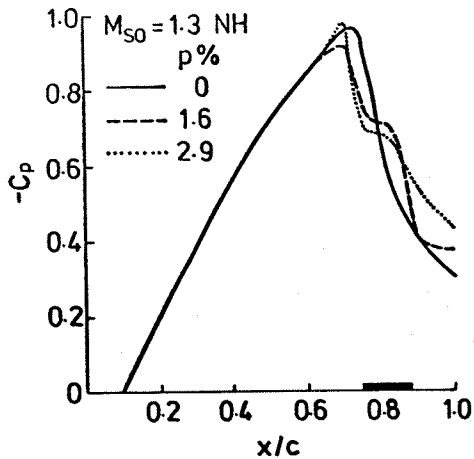


Fig. 3(a) Effect of porosity on pressure distribution - circular arc model.

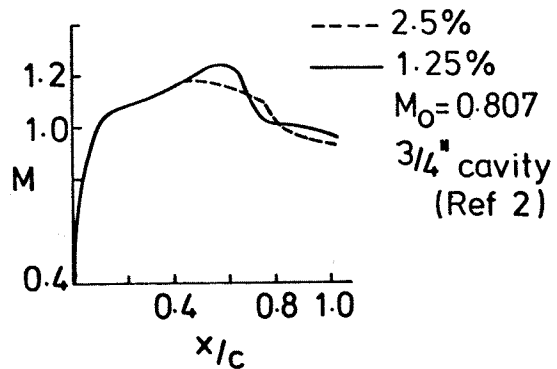


Fig. 3(b) Effect of porosity on Mach number distribution supercritical aerofoil.

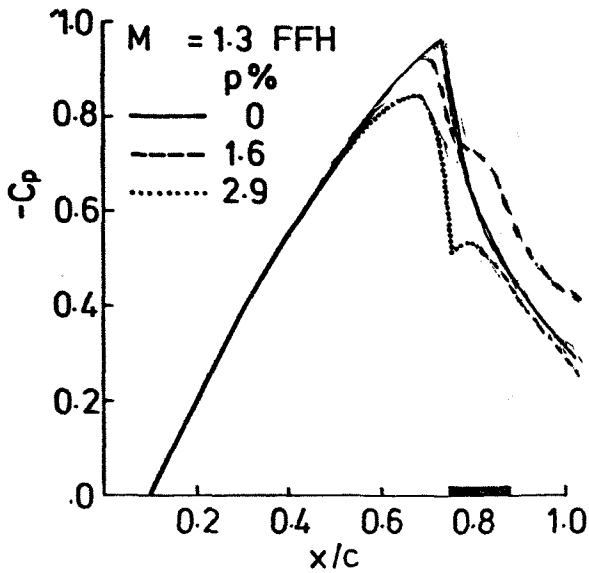


Fig. 3(c) Effect of porosity on pressure distribution circular arc model. Forward facing holes.

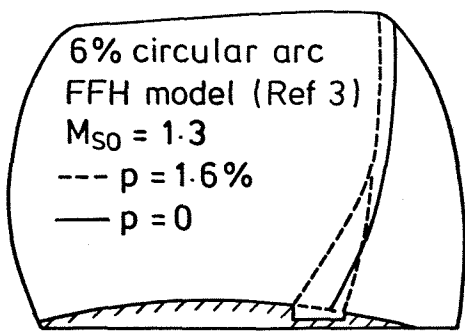


Fig. 4(a) Effect of porosity on shock wave. circular arc model - forward Facing holes.

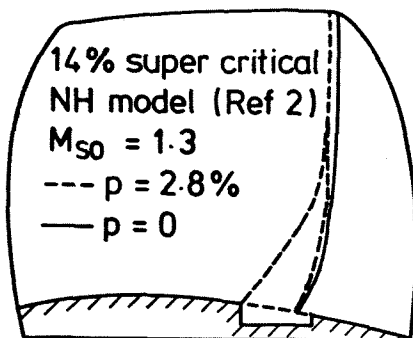


Fig. 4(b) Effect of porosity on shock wave. supercritical aerofoil - normal holes.

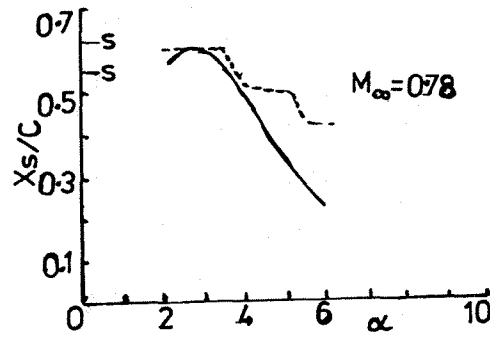


Fig. 4(c) Effect of PSBL control on shock position; supercritical aerofoil slotted model. (S - position of slots)

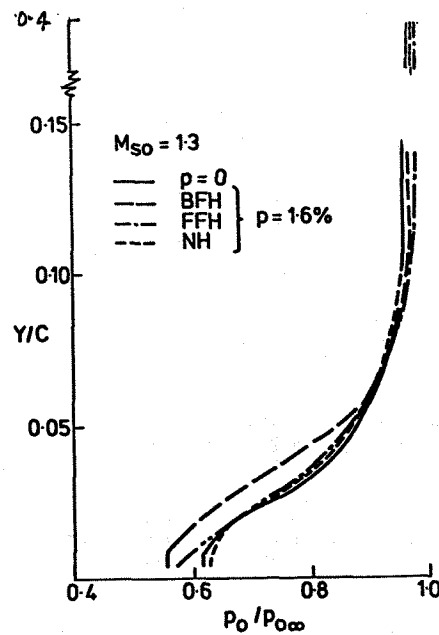


Fig. 5(a) Total pressure profiles 10% chord downstream of the trailing edge - circular arc model.

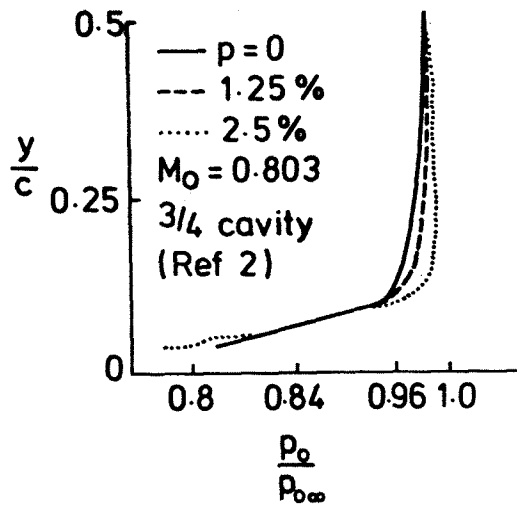


Fig. 5(b) Total pressure profiles in the wake - supercritical aerofoil model - normal holes.

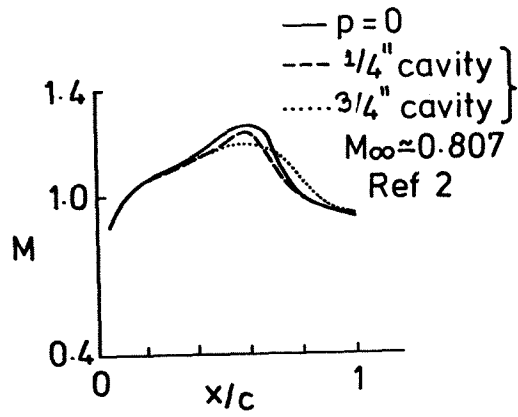


Fig. 8 Effect of cavity depth on Mach number distribution - supercritical aerofoil model. ( $p = 2.5\%$ )

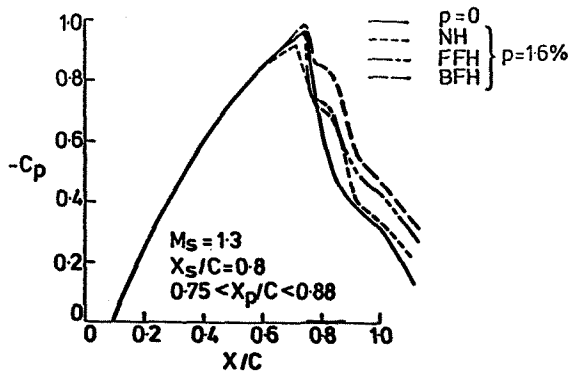


Fig. 6. Effect of hole inclination on pressure distribution - circular arc model.

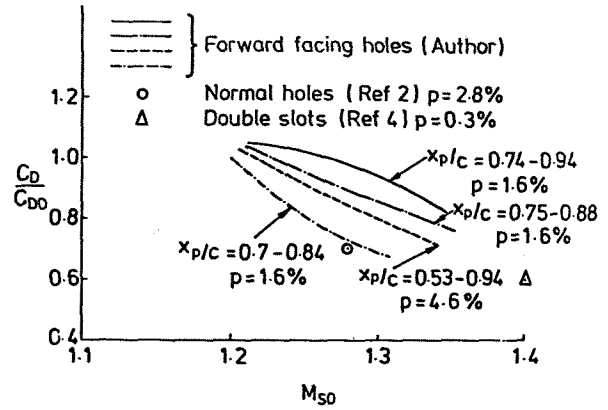


Fig. 9. Effect of porosity on its relative position on drag.

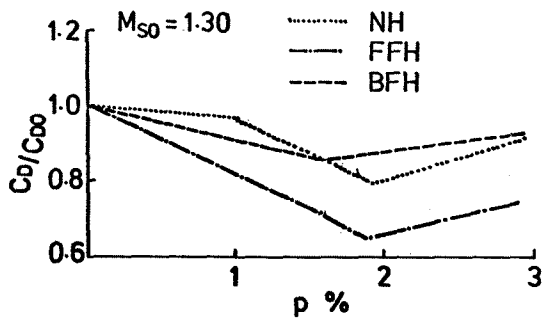
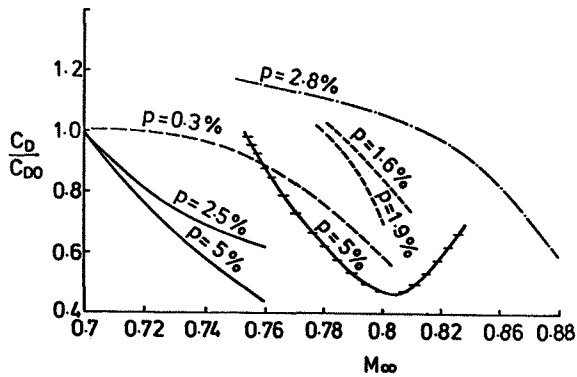


Fig. 7. Effect of hole inclination on drag - circular arc model.  $x_p/c = 0.7 - 0.84$ .



- Based on prediction. NACA 0012. Type C porosity (Ref 7)
- Based on prediction. NACA 0012. Type B porosity (Ref 7)
- Experimental supercritical. Double slots (Ref 4)
- Experimental, wall mounted circular arc, FF holes Type A (Ref 3)
- Experimental wall mounted supercritical N holes Type A (Ref 2)

Fig. 10. Effect of type of porosity distribution on drag reduction.

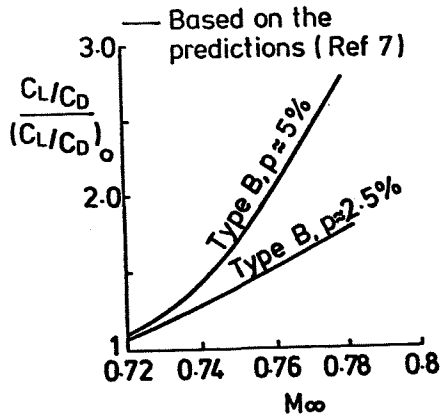


Fig. 11. Effect of PSBL control on lift to drag ratio. (Potential flow)

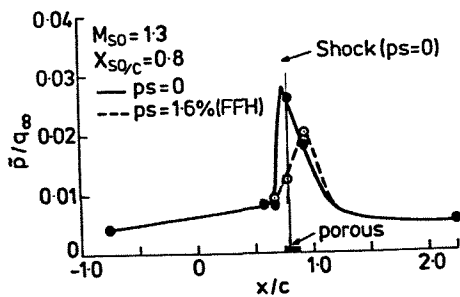


Fig. 12. Pressure fluctuations in the shock boundary layer interaction circular arc model.

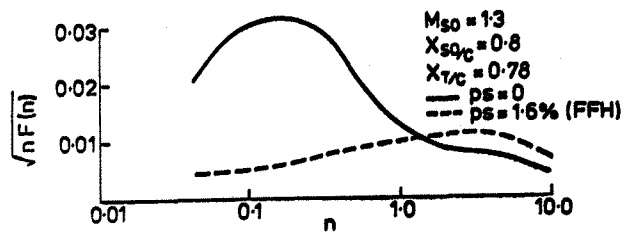


Fig. 13(a) Spectra of pressure fluctuations at the shock position.

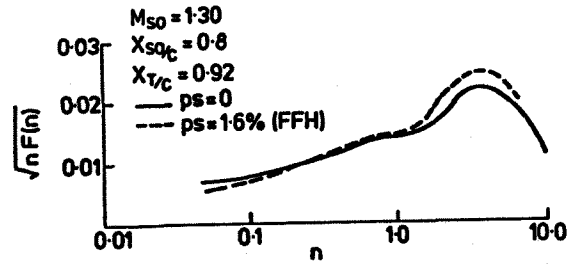


Fig. 13(b) Spectra of pressure fluctuations in the separated flow.

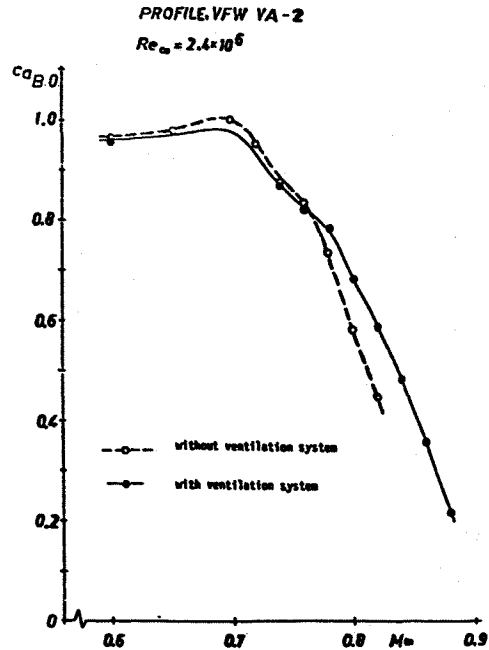


Fig. 14. Effect of PSBL control on buffet boundaries. Slotted model based on Ref. 4 and Ref. 5.